REE distributions in tourmaline: An INAA technique involving pretreatment by B volatilization

Robert W. King, Robert W. Kerrich

Department of Geological Sciences, University of Saskatchewan, Saskatoon S7N 0W0, Canada

Robin Daddar

Department of Geology, The University of Western Ontario, London, Ontario N6A 5B7, Canada

Abstract

The determination of trace-element and rare-earth-element abundances in tourmaline and other B-rich minerals by INAA analysis is hampered by the problem of incident neutron-flux suppression in the sample, arising from the intrinsically large neutron-capture cross section of B. Using a novel wet-chemical technique involving pretreatment by B volatilization, trace-element and REE abundances in tourmalines from gold-bearing vein deposits of the Superior province are reported. Abundances of REEs in tourmaline determined only by instrumental neutron-activation analysis are on average lower by a factor of 60%, as a consequence of the neutron-capture effect, compared to INAA results obtained on samples that have undergone the wet-chemical pretreatment. Total abundances after pretreatment range from less than detection to in excess of $\Sigma REE = 167$ ppm. The REE contents do not correlate with the levels anticipated in contiguous host rocks. This result indicates that the REE are only partially indigenous to wall rocks and suggests some transport of the REE in hydrothermal solutions.

Introduction

Tourmaline is the most common of the borosilicate minerals, occurring in many rock types and geologic environments. Hydrothermal tourmalines are known principally from (1) granitoid-associated mineralization (Power, 1968; Neiva, 1974; Clarke, 1981; Charoy, 1982), (2) gold-bearing vein deposits of Archean greenstone belts (Fleischer and Routhier, 1973; Kerrich, 1983; King et al., 1986; King and Kerrich, 1986a, 1986b), and (3) sporadic occurrences in stratabound, polymetallic, massive sulfide deposits (Ethier and Campbell, 1977; Taylor and Slack, 1984). Tourmaline also occurs not only as a detrital mineral in sedimentary rocks (Krynine, 1946; Pettijohn et al., 1973), but also develops authigenically during the late stages of diagenesis (Awasthi, 1981; Gautier, 1979). In addition, tourmaline has been found in metamorphic rocks encompassing a wide range of bulk compositions and develops at virtually all grades of metamorphism.

The distinctive compositions of hydrothermal tourmalines from different geologic environments (Clarke, 1981; Taylor and Slack, 1984; King and Kerrich, 1986a, 1986b) raises the possibility that characteristic variations in the distribution of trace elements may also exist. In this paper, we report trace-element abundances of tourmalines from gold-bearing vein deposits of the Superior province, Canada, with emphasis on REE distributions. Data have been obtained using a novel technique involving pretreatment to volatilize B and so circumvent the high neutron-flux suppression that would otherwise occur because of the large neutron-capture cross section of this element.

Knowledge of the REE contents of tourmaline has a critical bearing on many aspects of its genetic development. Precise age determinations based on Sm-Nd mineral isochrons are possible if abundances of REE and relative fractionations of Sm/Nd are sufficiently high in tourmaline and coexisting minerals (Fryer and Taylor, 1984): isotopic "tracing" of source reservoirs for the B-rich fluids is then possible from initial Nd-isotope ratios. Distributions of the REE can provide evidence for the dominant REE complexing ligands in solution, given the differing stabilities of the various REEs to Cl^-, F^-, and CO_3^{2-} complexes (Taylor and Fryer, 1983). Moreover, the magnitude of Eu anomalies may be used to monitor the redox state of hydrothermal fluids (Kerrich and Fryer, 1979; Clark, 1984). Finally, the provenance of specified trace elements—i.e., the extent to which the REEs are donated by wall rocks or alternatively are indigenous to the hydrothermal fluids—can be assessed by analysis of tourmalines in veins traversing different rock types.

Samples

Tourmalines analyzed in this study were collected from gold-bearing vein deposits in the Abitibi subprovince of the Superior province, Canada. Veins are typically com-

TABLE 1. Neutron-capture cross sections for the most abundant isotopic species of the major chemical elements in tourmaline

Nuclide	Isotopic abundance	Cross section (barns)
${}^{1}_{1}H$	99.98	0.332
${}^{7}_{3}Li$	92.5	0.045
${}^{10}_{5}B$	19.8	0.5
		3838 (n,α)
${}^{11}_{5}B$	80.2	0.005
${}^{16}_{8}O$	99.76	1.78×10^{-4}
${}^{19}_{9}F$	100	0.0096
${}^{23}_{11}Na$	100	0.10
${}^{24}_{12}Mg$	78.99	0.053
${}^{27}_{13}Al$	100	0.231
${}^{28}_{14}Si$	92.23	0.17
${}^{40}_{20}Ca$	96.94	0.41
${}^{48}_{22}Ti$	73.7	8.3
${}^{55}_{25}Mn$	100	13.3
${}^{56}_{26}Fe$	91.8	2.6

Note: Source of data. Brown et al. (1978). Values listed are thermal neutron-capture cross sections ($\sigma_c = \sigma(n,\gamma)$), except where indicated as $\sigma(n,\alpha)$, in units of barns (10^{-24} cm²).

TABLE 2. Residual B abundance in solution after chemical treatment

Sample	Mine	B ($\mu g/mL$)
T1	Dome	0.51
T2	Lamaque	0.04
T3	Bras D'Or	0.04
T4	Deep Dome	0.30
T6	Bousquet	0.24
T7	Pascalis	0.10
T10	Middleton Lake	1.76
T11	Matachewan Consolidated	0.46

posed of quartz, calcite, ferroan dolomite, tourmaline, muscovite, paragonite, chlorite, pyrite, and gold. Tourmaline is generally present as a trace constituent, but may form up to 80% of some veins. In order to explore the possible influence of wall rocks on the trace-element content of tourmalines, veins were sampled from a wide variety of geologic environments and host rocks, including ultramific volcanic rocks (Dome mine), tholeiitic basalt (Noranda), granodiorite (Lamaque, Bras D'Or), trondhjemite (Deep Dome), rhyolite (Bousquet), and syenite (Matachewan Consolidated). Details of the locations, textures, mineralogy, and geologic settings of the tourmaline-bearing veins are given in King et al. (1986) and Kerrich (1983). In order to minimize the problem of possible trace-element variations at microscopic levels, samples were selected from a larger population of tourmaline-bearing veins that had been screened by electron microprobe for compositional uniformity and lack of zoning. For purposes of convenience, we confine this study to one type of hydrothermal tourmaline occurrence; work is in hand to determine REE characteristics of tourmalines from other geologic environments.

B INTERFERENCE

The determination of trace-element abundances in tourmaline and other B-rich minerals by INAA is affected by a suppression of the incident neutron flux in the target sample during irradiation, arising from the intrinsically large neutron-capture cross section of boron. The production rate R of a nuclide for an irradiation with thermal neutrons is defined as

$$R = Na\sigma F, \qquad (1)$$

where N is the number of target atoms of a particular *element* in the irradiated sample, a is the isotopic abundance of the target *isotope,* σ is the neutron-capture cross section in barns of the target nuclide, and F is the neutron flux in units of neutrons per square centimeter per second (Faure, 1977, p. 58). It is clear that if the incident neutron flux is significantly suppressed, the production rate R and ensuing γ activity of irradiated nuclides in the sample will diminish. Accordingly, analytical discrepancies will arise because activities of isotopes induced in a B-rich sample compared with standards will vary not only with concentration, but also with the degree of flux suppression induced by B content.

The thermal neutron-capture cross section of ${}^{10}_{5}B$ is small, being of the same order as for other major elements: Na, Al, Si, Ca, and Fe. However, ${}^{10}_{5}B$ is characterized by a large neutron-capture cross section for the reaction

$$ {}^{10}_{5}B + n \rightarrow {}^{7}_{3}Li + {}^{4}_{2}He. \qquad (2) $$

Values for B, together with the other major cations and anions present in tourmaline, are listed in Table 1.

The problem of neutron-flux suppression could potentially be resolved by doping standards with B contents equivalent to that in the unknowns, but in the absence of precise B determinations for each unknown, this quantity is generally only an estimate. Moreover, dopant addition raises the problem of reagent contamination. As an alternative approach, we report a wet-chemical technique involving B volatilization prior to INAA and demonstrate that this technique is capable of overcoming the systematically low abundances of the REE obtained on untreated samples of tourmaline by conventional INAA.

ANALYTICAL METHODS

Tourmalines were separated using a combination of the Franz isodynamic magnetic separator and heavy liquids (sodium polytungstate [$3Na_2WO_4:9WO_3:H_2O$], density 2.8 g/cm³). All separates were checked for contaminants both visually and by X-ray diffraction and are considered to be better than 99% pure.

Tourmaline separates were then decomposed using a modified standard wet-chemical technique for silicates, but using a Teflon bomb to overcome the resistance of tourmaline to digestion in boiling hydrofluoric acid (HF) at atmospheric pressure. Aliquots of tourmaline (250 mg),

TABLE 3. Representative microprobe analysis of tourmaline

	T1	T2	T3	T4	T6	T7	T10	T11	T12
SiO_2	37.04	37.53	35.94	37.44	37.03	37.97	37.04	35.92	36.05
Al_2O_3	33.77	31.92	31.77	33.15	31.22	32.93	30.41	28.71	31.55
B_2O_3*	10.85	10.85	10.85	10.85	10.85	10.85	10.85	10.85	10.85
FeO	9.91	6.78	8.38	6.57	6.18	6.85	11.62	12.82	7.96
MnO	0.02	0.00	0.05	0.01	0.01	0.04	0.04	0.02	0.03
CaO	0.09	0.043	0.28	0.23	1.26	0.32	0.13	0.34	0.54
Na_2O	1.72	2.34	2.25	2.29	2.06	2.07	2.79	2.78	2.38
MgO	3.65	7.44	6.02	6.35	8.11	6.78	6.41	5.27	6.35
K_2O	0.02	0.00	0.00	0.00	0.00	0.01	0.05	0.02	0.01
TiO_2	0.70	0.31	0.44	0.40	0.36	0.15	0.36	0.49	0.66
Cr_2O_3	0.12	0.00	0.07	0.08	0.01	0.06	0.05	0.06	0.13
Total	97.89	97.60	96.05	97.37	97.09	98.02	99.75	97.28	96.51
				Structural formula on the basis of 29 oxygens					
B	3.000	3.000	3.000	3.000	3.000	3.000	3.000	3.000	3.000
Si	6.014	6.062	5.943	6.042	6.015	6.092	6.010	6.015	5.935
Al_T	0.000	0.000	0.057	0.000	0.000	0.000	0.000	0.000	0.065
Al_Z	6.000	6.000	6.000	6.000	5.979	6.000	5.818	5.669	6.000
Al_Y	0.465	0.078	0.136	0.307	0.000	0.227	0.000	0.000	0.059
Ti	0.085	0.038	0.055	0.049	0.044	0.018	0.044	0.062	0.082
Fe	1.346	0.916	1.159	0.887	0.840	0.919	1.577	1.796	1.096
Mn	0.002	0.000	0.006	0.001	0.001	0.004	0.004	0.002	0.003
Mg	0.883	1.791	1.483	1.527	1.963	1.621	1.550	1.315	1.558
Cr	0.015	0.000	0.009	0.010	0.003	0.008	0.006	0.008	0.017
Y total	2.796	2.823	2.848	2.781	2.851	2.797	3.181	3.183	2.815
Ca	0.016	0.074	0.050	0.040	0.219	0.055	0.023	0.061	0.095
Na	0.542	0.733	0.721	0.716	0.649	0.644	0.878	0.903	0.760
K	0.004	0.000	0.000	0.000	0.000	0.002	0.010	0.004	0.002
X total	0.562	0.807	0.771	0.756	0.808	0.701	0.911	0.968	0.857

Note: T1 = Dome; T2 = Lamaque; T3 = Bras D'Or; T4 = Deep Dome; T6 = Bousquet; T7 = Pascalis; T10 = Middleton Lake; T11 = Matachewan Consolidated; T12 = Noranda.
* B assumed to be stoichiometric.

comminuted to a particle size of ≤ 100 μm, were decomposed with HF in a Teflon bomb at a temperature of 220 °C over a duration of 24 h. The digestate was transferred quantitatively to a Teflon beaker, 2 mL of nitric acid (HNO_3) was added, and the solution was evaporated to dryness. B is volatilized during this stage of the chemical treament. Percholoric acid ($HClO_4$) (2 mL) was then added and slowly evaporated to dryness over a period of approximately 10 h. The residue was taken into solution with 1 mL of concentrated hydrochloric acid (HCl), fol-

TABLE 4. Abundances of the REE and selected trace elements in specified tourmalines and standard (ppm)

	Treated T3	Raw T3A	Treated T6	Raw T6A	Treated T7	Raw T7A	Treated			
							T1	T2	T4	T10
La	0.6	0.05	15.1	10.9	5.5	3.6	28.9	0.8	1.0	1.4
Ce	1	1	32	27	15	8	65	1	2	3
Nd	<3	<3	19	15	8	5	31	<3	<3	1.79
Sm	0.18	0.14	4.47	3.57	1.80	1.33	5.71	0.07	0.27	0.27
Eu	<0.18	0.05	0.49	0.38	0.44	0.29	1.83	<0.11	0.23	0.32
Tb	0.11	0.01	0.6	0.5	0.3	0.2	0.5	<0.1	0.11	0.1
Dy	1.2	0.7	4.5	3.4	1.7	1.1	2.3	1.2	1.6	0.7
Yb	0.17	0.13	3.65	2.85	1.18	0.78	2.55	<0.14	1.20	0.20
Lu	0.03	0.02	0.67	0.53	0.15	0.11	0.47	0.01	0.20	0.03
Sc	42	30.8	42.8	32.1	61.0	39.3	162	18.6	60.7	28.0
Sr	825		59.9		247		37.8	731	414	—
Th	<0.1	0.1	1.7	1.4	0.3	0.3	1.4	0.4	<0.1	1.4
U	0.1	0.1	0.6	0.3	0.1	0.3	0.6	0.1	0.2	0.4
Zn	400	130	310	270	210	150	1700	800	330	460
La_{cn}/Yb_{cn}	2.4	2.6	2.8	2.6	3.1	3.1	7.7	4.5	0.6	4.7
Eu/Eu*	1.00	1.16	0.41	0.40	0.73	0.69	1.00	1.08	1.49	1.83
Sm/Nd	—	—	0.23	0.24	0.22	0.27	0.18	—	—	0.15
Sr/Eu	—	—	122	—	561	—	20.7	—	1800	—
ΣREE	4.7	3.6	94	75	38	24	167	4.7	11	10

Note: T1 = Dome; T2 = Lamaque; T3 = Bras D'Or; T4 = Deep Dome; T6, T6A = Bousquet; T7, T7A = Pascalis; T10 = Middleton Lake; T11 =

lowed by 10 mL of $0.5M$ HCl. The resulting solution was transferred to a polythene liner supported in a 100-mL polypropylene beaker and evaporated to dryness in a vacuum oven at a temperature of 70 °C and ~300 millitorr. Following complete evaporation of the solutions, the polythene liners were inserted into standard 2-mL irradiation capsules for INAA. An "in house" granite standard (UWO-1) was processed by the same wet-chemical pretreatment as the tourmalines to assess quantitative recovery of the REE. Three "raw" tourmalines were analyzed together with their treated counterparts to evaluate the magnitude of analytical differences arising from the presence of B. Instrumental neutron activation analysis was done courtesy of E. Hoffman of Nuclear Activation Services Limited.

For the determination of B in solution, a separate 250-mg aliquot of tourmaline was decomposed as above, evaporated to dryness, taken to 25 mL, and analyzed for B by inductively-coupled plasma-emission spectroscopy (ICP). Detection limits were 40 ng/mL in solution, corresponding to 4 μg/g (4 ppm) referenced to the powdered tourmaline.

Electron-microprobe analyses of tourmalines were done on a three-spectrometer MAC-400 electron microprobe with KRISEL automation (Finger and Hadidiacos, 1972) and appropriate natural mineral standards. The data were reduced on line with the MAGIC IV reduction program (Colby, 1971).

RESULTS

B volatilization

In order to test the efficiency of B volatilization during chemical pretreatment, B was determined in solutions

TABLE 4—Continued

	Treated		Treated	Raw
	T11	T12	UWO-1	UWO-1
	1.6	1.8	38.4	46
	4	5	80	
	3	4	36	38
	1.03	1.28	7.18	8.6
	0.56	0.42	0.81	1.10
	0.4	0.3	1.0	1.13
	2.9	1.8	4.5	
	1.52	1.10	3.46	4.00
	0.24	0.19	0.60	0.60
	93.2	29.5	5.68	6.97
	—	—	—	—
	0.2	0.1	21	22
	0.1	0.2	8.8	
	<5	120	51	
	0.7	1.1	7.5	7.8
	1.07	0.83	0.41	0.47
	0.34	0.32	0.20	
	—	—	—	—
	21	21	190	202

Matachewan Consolidated; T12 = Noranda; UWO-1 granite standard.

prepared after the perchloric acid evaporation stage. Data for the B content of decomposed tourmalines in solution are reported in Table 2. Solute concentrations of B range from 1.76 to <0.04 μg/mL, corresponding to a maximum of 176 μg/mL (ppm) when referenced to the starting mineral. Given B contents of tourmalines of approximately ~10.8 wt% B_2O_3 (Deer et al., 1982), or ~3×10^4 μg/g B, it is clear that B is essentially completely volatilized during the wet-chemical pretreatment of the tourmalines.

Trace-element content

Electron-microprobe analyses of the nine tourmalines are reported in Table 3, with the corresponding trace-element data compiled in Table 4. It is clear from inspection of Table 4 that the concentrations of the REE and other trace elements in the untreated tourmaline separates are systematically lower than in their pretreated counterparts, by an average 60%. REE profiles of untreated tourmaline and pretreated equivalents track one-another in each of the three pairs analyzed in both modes, such that the recorded differences are present over the full range of atomic number from La to Lu (Figs. 1A–1C). This systematic disparity extends to the other trace elements determined by INAA, including Sc, Th, Hf, and U (Table 4), endorsing the necessity of removing B from B-rich minerals prior to INAA.

In the suite of tourmalines, significant variations exist both in the absolute abundance of REEs and in their chondrite-normalized distributions (Figs. 1 and 2). Total REE contents span more than two orders of magnitude. The maximum recorded abundance is present in T1, in which REE = 167 ppm (ΣREE calculated according to the procedure of Cullers and Graf, 1984). Tourmalines from Bousquet (T6, ΣREE = 95 ppm), Bras D'Or (T7, ΣREE = 38 ppm), and Matachewan Consolidated (T11, ΣREE = 21 ppm) record progressively lower absolute REE contents, whereas in sample T2 from Lamaque, ΣREE $\leq$ 5 ppm, and in several members of the group the REEs are below detection limits (Figs. 1 and 2).

In terms of REE distributions, T1 has a moderately fractionated pattern (chondrite-normalized La/Yb = 7.7) with a monotonic decrease from La to a minimum at Dy, followed by a systematic upturn in the HREE, to Lu (Fig. 2A). Tourmaline from Bousquet (T6) is somewhat less fractionated (chondrite-normalized La/Yb = 2.8), with smoothly diminishing chondrite-normalized values from La to Tb, but with a pronounced intervening negative Eu anomaly (Eu/Eu* = 0.4); an upturn of the HREE is also evident in this sample. A similar pattern is present in another separate from Bras D'Or (T3), which is characterized by a minimum in the region of Tb-Dy, but no Eu anomaly (Fig. 1C).

Three of the tourmalines (T7, T11, T12) possess slightly fractionated to flat patterns, where chondrite-normalized La/Yb = 3.1, 0.7, and 1.1, respectively (Figs. 1B, 2B). The remaining two tourmalines have positive (T2)
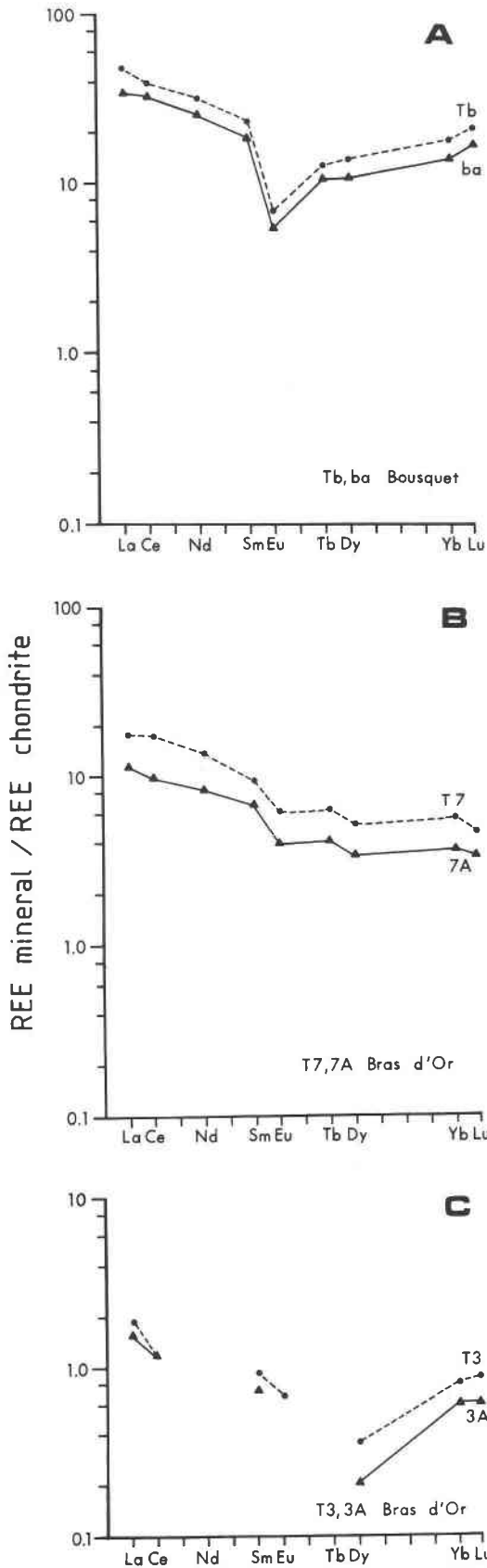
Fig. 1. Chondrite-normalized REE distribution for specified tourmaline and their pretreated counterparts (lower dashed lines). (A) Bousquet; (B) Bras D'Or, T7; (C) Bras D'Or, T3.
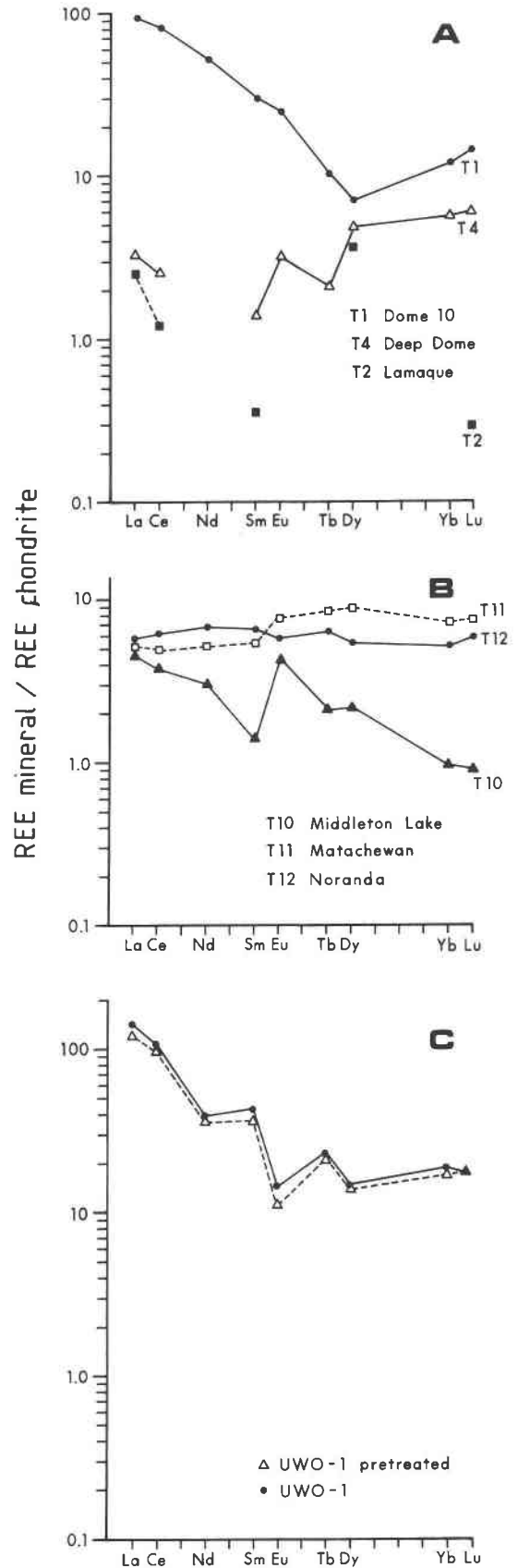
Fig. 2. Chondrite-normalized REE distributions for (A and B) specified tourmalines and (C) UWO-1 standard granite and its treated counterpart.

and negative (T10) slopes, respectively, with multiple maxima and minima in T2 (Figs. 2A, 2B).

Of the additional trace elements reported in Table 3, Sc [maximum = 162 ppm, $\bar{x} = 47 \pm 40$ (1σ)] is present at appreciable levels in the majority of tourmalines, whereas abundances of Th, U, and Hf are in the low ppm range in all samples.

DISCUSSION

Method

The observation of systematically diminished analytically determined abundances of the REE, together with other trace elements, in raw tourmalines (untreated) relative to chemically pretreated equivalents is most simply interpreted in terms of the large neutron-captive cross section of B. This conclusion is supported by the fact that most sources of interference in INAA are element specific and would not be expected to act systematically over the entire array of elements analyzed here. The large neutron-capture cross section of $^{10}_{5}$B is anticipated to suppress the incident neutron flux, thereby partially shielding all nuclides subject to neutron capture and diminishing their rate of activation. This study demonstrates that the neutron-capture interference effect cannot be ignored in precise analytical studies of B-rich minerals by INAA.

The general case of self-shielding of neutrons during irradiation as a result of high concentrations of an isotope with very high neutron-capture cross section has been reviewed by De Soete et al. (1972, p. 457). Potts has calculated the following concentrations of elements necessary to induce a 1% flux depression caused by self-absorption of neutrons: Gd, 36 ppm; B, 150 ppm; Sm, 280 ppm; Eu, 370 ppm; and Cd, 480 ppm (Potts, 1987, p. 427). These theoretical results are in keeping with the experimental data reported here, demonstrating diminished analytically determined abundances due to suppression of the incident-neutron flux in B-rich minerals.

The wet-chemical pretreatment, which exploits the relatively high volatility of B even at low temperatures, is clearly effective in the near total removal of this element from solutions prior to INAA. At the same time, the REE, together with Sc, Th, U, and Zn, are almost completely recovered during the wet-chemical procedure, as indicated by the agreement of results for the granite standard and a pretreated aliquot (UWO-1, Table 4; Fig. 2C). The majority of analytical results for the treated granite are within one standard deviation of replicate analyses of the standard, and all results are within two standard deviations.

Decomposition of tourmaline with HF in a Teflon bomb is preferred over the use of alkali-metal carbonate fluxes, to circumvent the introduction of possible reagent contaminants and to avoid dilution effects.

Geologic significance

Variations in the REE distribution in minerals are controlled by crystal-chemical and/or geochemical factors. Tourmaline has a general formula $XY_3Z_6(BO_3)_3Si_6O_{18}$-$(OH)_4$. The X site commonly contains Na but may also accommodate variable amounts of Ca, Mg, and vacancies (Foit and Rosenberg, 1977). The Y site tolerates extensive and diverse substitutions involving monovalent, divalent, trivalent, and quadrivalent cations (Frondel et al., 1966; Herman et al., 1973; Fortier and Donnay, 1975; Foit and Rosenberg, 1979). The Z site usually contains Al but significant amounts of Fe^{2+}, Fe^{3+}, Ti, Mg, Cr, and V^{3+} can replace Al (Barton, 1969; Tsang et al., 1971; Gorelikova et al., 1978; Foit and Rosenberg, 1979; Korovushkin et al., 1979; Nuber and Schmetzer, 1979).

According to Clark (1984), minerals with high coordination numbers (>9) for their REE sites are Ce selective, whereas those with coordination number 6 are Y selective; minerals with intermediate coordination numbers (7–9) have complex REE distributions. The variety and complexity of REE profiles observed in this study may indicate that tourmaline is characterized by REEs occupying sites with intermediate coordination numbers but this hypothesis requires further detailed work.

REE contents of these schorl-dravite tourmalines span two orders of magnitude, but there is no obvious dependence on composition, suggesting that paragenetic conditions are the predominant control on REE abundances. Inasmuch as the REE abundances and distributions in the tourmalines do not reflect those anticipated in the wall rocks, it is presumed that the REE have been inherited largely from the hydrothermal (sensu lato) solutions. For example, T1, which has the highest REE content of the suite of samples analyzed in this study, is hosted by ultramafic rocks, whereas samples in syenitic rocks (T10, T11) have relative low abundances of the REE. This result is in keeping with the provinciality of tourmaline REE characteristics (Figs. 1, 2), as well as with independent evidence for their precipitation under conditions of ambient high water/rock ratio (Kerrich, 1983).

A major complicating factor in interpreting the REE distributions of tourmaline is the unknown extent to which REEs are partitioned between competing coexisting phases. With the present limited data, this question is difficult to answer. We note, however, that T2, T3, and T7, which have different chondrite-normalized patterns, are all from similar paragenetic associations in which tourmaline is dominant; thus for these examples, partitioning may not be a first-order effect.

The position of chondrite-normalized Eu values with respect to the neighboring REEs variously generates negative (T6), zero (T1, T11, T12), and positive (T10) anomalies (Figs. 1, 2). Sr^{2+} and Eu^{2+}, which show similar geochemical behavior (Henderson, 1984) are not correlated in the tourmalines, suggesting that Eu may be present predominantly in the trivalent state. Further work is nec-

essary to assess whether such anomalies are mediated by the redox state, as determined from independent criteria.

For the majority of samples, Sm and Nd are present at levels well in excess of that required for precise isotopic analysis. Sm/Nd ratios are relatively uniform at 0.24 ± 0.06 (1σ). Accordingly, tourmaline satisfies all of the criteria necessary for its incorporation in a Sm-Nd mineral isochron, and further work is in hand on this topic. A feature common to many of the profiles is the upturn in the HREE region. Kerrich and Fryer (1979) noted this in bulk analyses of tourmaline-bearing veins and raised the possibility that enhanced levels of the HREE were due to their complexing by CO_3^{2-} in solution.

ACKNOWLEDGMENTS

REFERENCES CITED

Awasthi, N. (1981) Authigenic tourmaline and zircon in the Vindhyan formations of Some Valley, Mizapur District, Uttar Prandesh, India. Journal of Sedimentary Petrology, 31, 482–484.

Barton, R., Jr. (1969) Refinement of the crystal structure of buergerite and absolute orientation of tourmalines. Acta Crystallographica, B25, 1524–1532.

Brown, E., Dairiki, J.M., Doebler, R.E., Shihab-Eldin, A.A., Jardine, L.J., Tuli, J.K., and Buyrn, A.B. (1978) Table of isotopes. Wiley, New York.

Charoy, P. (1982) Tourmalinization in Cornwall, England. In A.M. Evan, Ed., Mineralization associated with acid magmatism, p. 63–70. Wiley, New York.

Clark, A.M. (1984) Mineralogy of the rare earth elements. In P. Henderson, Ed., Rare earth element geochemistry, p. 33–61. Elsevier, Amsterdam.

Clarke, D.B. (1981) The mineralogy of peraluminous granites. A review. Canadian Mineralogist, 19, 3–17.

Colby, J.W. (1971) MAGIC IV, a computer program for quantitative electron microprobe analysis. Bell Telephone Laboratories, Allentown, Pennsylvania, U.S.A.

Cullers, R.L., and Graf, J.L. (1984) Rare earth elements in igneous rocks of the continental crust: Predominantly basic and ultrabasic rocks. In P. Henderson, Ed., Rare earth element geochemistry, p. 237–273. Elsevier, Amsterdam.

Deer, W.A., Howie, R.A., and Zussman, J. (1982) Rock-forming minerals, Vol. 1, Ortho- and ring silicates (fourth edition), p. 300–319. Wiley, New York.

DeSoete, D., Gijbels, R.J., and Hosk, J. (1972) Neutron activation analysis. Wiley, London.

Ethier, V.G., and Campbell, F.A. (1977) Tourmaline concentrations in Proterozoic sediments of the southern Cordillera of Canada and their economic significance. Canadian Journal of Earth Sciences, 14, 2345–2363.

Faure, G. (1977) Principles of isotope geology. Wiley, Toronto.

Finger, L.W., and Hadidiacos, C.G. (1972) Electron microprobe automation. Carnegie Institution of Washington, Geophysical Laboratory Annual Report, 71, 598–600.

Fleischer, R., and Routhier, P. (1973) The "consanquineous" origin of a tourmaline-bearing gold deposit: Passagem de Mariana (Brazil). Economic Geology, 68, 11–22.

Foit, F.F., Jr., and Rosenberg, P.E. (1977) Coupled substitutions in the tourmaline group. Contributions to Mineralogy and Petrology, 62, 109–127.

——— (1979) The structure of vanadium-bearing tourmaline and its implications regarding tourmaline solid solutions. American Mineralogist, 164, 788–798.

Fortier, S., and Donnay, G. (1975) Schorl refinement showing composition dependence of the tourmaline structure. Canadian Mineralogist, 13, 173–177.

Frondel, C., Biedl, A., and Ito, J. (1966) New type of ferric iron tourmaline. American Mineralogist, 51, 1501–1505.

Fryer, B.J., and Taylor, R.P. (1984) Sm-Nd direct dating of the Collins Bay hydrothermal uranium deposit, Saskatchewan. Geology, 12, 479–482.

Gautier, D.L. (1979) Preliminary report of authigenic euhedral tourmaline crystals in a productive gas reservoir of the Tiger Ridge Field, north-central Montana. Journal of Sedimentary Petrology, 49, 911–916.

Gorelikova, N.V., Perfil'yev, Yu.D., and Bubeshkin, A.M. (1978) Mossbauer data on distribution of Fe ions in tourmaline. International Geology Review, 20, 982–990.

Henderson, P. (1984) General geochemical properties and abundances of the rare earth elements. In P. Henderson, Ed., Rare earth element geochemistry, p. 1–32. Elsevier, Amsterdam.

Herman, E., Simkin, D.J., Donnay, G., and Muir, W.B. (1973) The distribution of Fe^{2+} and Fe^{3+} in iron-bearing tourmalines: A Mossbauer study. Tschermaks Mineralogische und Petrographische Mitteilungen, 19, 124–132.

Kerrich, R. (1983) Geochemistry of gold deposits in the Abitibi greenstone belt. Canadian Institute of Mining Special Paper 27, 75 p.

Kerrich, R., and Fryer, B.J. (1979) Archean precious metal hydrothermal systems, Dome mine, Abitibi greenstone belt II. REE and oxygen isotope relations. Canadian Journal of Earth Sciences, 16, 440–458.

King, R.W., and Kerrich, R. (1986a) Tourmaline in Archean lode gold deposits: I. Geochemical characteristics. Geological Society of America Abstracts with Programs, 18, 657.

———(1986b) Tourmaline in Archean lode gold deposits: II. REE distribution and Sr isotope characteristics. Geological Society of America Abstracts with Programs, 18, 657.

King, R.W., Kerrich, R., and Hoffman, E. (1986) Tourmaline geochemistry in Archaen lode gold deposits (abs.). In Poster volume of gold '86, International Symposium on the Geology of Gold, Toronto, 1986, 86–88.

Korovushkin, V.V., Kuzmin, V.L., and Below, V.F. (1979) Mossbauer studies of structural features in tourmaline of various geneses. Physics and Chemistry of Minerals, 4, 209–220.

Krynine, P.D. (1946) The tourmaline group in sediments. Journal of Geology, 54, 65–87.

Neiva, A.M.R. (1974) Geochemistry of tourmaline (schorlite) from granites, aplites and pegmatites from northern Portugal. Geochimica et Cosmochimica Acta, 38, 1307–1317.

Nuber, B., and Schmetzer, K. (1979) The lattice position of Cr^{3+} in tourmaline: Structural refinement of a chromium-rich Mg-Al-tourmaline. Neues Jahrbuch für Mineralogie Abhandlungen, 137, 184–197.

Pettijohn, F.J., Potter, P.E., and Siever, R. (1973) Sand and sandstones. Springer-Verglag, New York.

Potts, P.J. (1987) A handbook of silicate rock analysis. Blackie & Son Ltd., Glasgow and London.

Power, G.M. (1968) Chemical variation in tourmalines from south-west England. Mineralogical Magazine, 36, 1078–1089.

Taylor, B.E., and Slack, J.F. (1984) Tourmalines from Appalachian-Cal-

edonian massive sulfide deposits: Textural, chemical and isotopic relationships. Economic Geology, 79, 1703–1726.

Taylor, R.P., and Fryer, B.J. (1983) Strontium isotope geochemistry of the Santa Rita porphyry copper deposit, New Mexico. Economic Geology, 78, 170–174.

Tsang, T., Thorpe, A.N., and Donnay, G. (1971) Magnetic susceptibility and triangular exchange coupling in the tourmaline mineral group. Journal of the Physics and Chemistry of Solids, 32, 1441–1448.